EFFECT OF RICE HUSK ASH SILICA ($RHASiO_2$) COMPOSITION TO THE PROPERTIES OF SAMARIUM-DOPED CERIA ELECTROLYTE

Zolhafizi Jaidi[1], Mohd Azham Azmi[1,*], Hamimah Abd Rahman[1], Mohd Faizal Tukimon[1], Muhammad Zul Idzham Abdul Ghani[1], Muhammad Syahmie Sufi Abdul Shukor[1] and Tan Kang Huai[2]

[1]Faculty of Mechanical and Manufacturing Engineering, Universiti Tun Hussein Onn Malaysia, 86400 Parit Raja, Batu Pahat, Johor, Malaysia.
[2]Department of Mechanical Engineering, Faculty of Engineering and Technology, Tunku Abdul Rahman University of Management and Technology, Jalan Genting Kelang, Setapak, 53300, Kuala Lumpur, Malaysia.

*azham@uthm.edu.my

Abstract. Commercial inclusion of ceramic oxides such as copper oxide, lithium oxide, and iron oxide into ceria-based electrolytes has been utilized to improve ceria-based material performance by microstructure modification. The purpose of this research is to investigate the impact of rice husk ash silica ($RHASiO_2$) composition on samarium-doped ceria electrolyte properties. This innovation, utilizing natural silica from rice husk ash, promotes eco-friendly technology development in engineering. $RHASiO_2$ was calcined for 4 hours at 700 °C to produce high purity silica, which was then mixed with SDC powder using a dry ball milling process. SDC0, SDC0.25, SDC0.5, and SDC1.0 will include 0%, 0.25%, 0.5%, and 1.0% $RHASiO_2$, respectively. To establish if $RHASiO_2$ may act as an addition to the electrolyte, all samples will be sintered at 1200 °C for 60 minutes. TGA analysis was used to describe the composite powder on the basis of thermal characteristics, and Archimedes' principle will be employed to determine the porosity and density of the composite pellet. When compared to the pure SDC electrolyte, the density of the electrolyte with a greater weight % of $RHASiO_2$ was higher. For SDC0.25, SDC0.5, and SDC1.0, the FTIR results clearly demonstrated $RHASiO_2$ bonding at 1088, 1066, and 1067 cm^{-1}, respectively, whereas 1104 cm^{-1} suggests an asymmetric stretching vibrations band. After the sintering process, the addition of silica will offer a new bonding element. EDX was used to identify the elements in the samples to establish the presence of SiO. Aside from that, SEM micrographs and Image J showed that the porosity percentage reduces when $RHASiO_2$ composition increases. Overall, the results of all investigations suggest that adding $RHASiO_2$ to SDC decreases its porosity while increasing the properties of the SDC-$RHASiO_2$ electrolyte composite.

Keywords: RHA, rice husk ash silica, ball milling, SDC, electrolyte, sintering aid

Article Info

Received 10th January 2024
Accepted 22nd May 2024
Published 12th June 2024

ISSN: 1823-7010, eISSN: 2600-7444

1. INTRODUCTION

It is commonly known that solid oxide fuel cells [1], or SOFCs for short, have a great deal of potential to be significant power sources in the future because of their high energy conversion efficiency, high electrolyte stability, longer stack life, and low pollutant emission. They can use a variety of fuels. Because oxygen anions (O^{2-}) behave as conducting species throughout the electrolytes to reach the anode side for the electrochemical interactions with any combustible fuel, a SOFC's primary benefit is its considerably higher versatility with realistic fuels [2-3].

Solid oxide electrolytes are a critical component of SOFC systems. In general, the essential issue to consider is the ionic conductivity of a solid oxide electrolyte. The most common SOFC electrolyte is yttria-stabilized zirconia (YSZ), which requires high operating temperatures (800-1000 °C) to maintain a high ionic conductivity (0.01 S/cm). However, at such high operating temperatures, YSZ as solid oxide electrolytes can produce significant materials challenges, such as mismatches in thermal expansion coefficients between ceramic components, electrode coking concerns, interfacial interdiffusion, and the possibility of cell sealing. Ceria-based solid solutions have been identified as the most promising electrolytes at intermediate temperatures (500-700 °C) SOFC (IT-SOFC) due to their higher ionic conductivity than YSZ [4-5].

In the manufacture of solid oxide electrolytes, powder pressing and sintering ceramic processes are widely utilized. After sintering as pressed pellets, current electrolytes exhibit structural difficulties such as non-uniform crystallite sizes, visible voids, and low bulk density. By using proper sintering aids and fine starting materials, electrolyte densification is increased, resulting in constant crystallite sizes and high-density solid electrolytes [6-7].

Ball-milling is a common process for manufacturing solid electrolytes, but it only produces micrometer-scale particle sizes and necessitates a much higher sintering temperature to produce highly dense pressed pellets. We demonstrated a milling method for fabricating fully-dense samarium-doped ceria (SDC) solid electrolytes using SiO_2 as sintering aids. To demonstrate how SiO_2 affects the densification behavior of ceria-based electrolytes, comparative research was carried out using a SDC system with SiO_2 addition. This information will be useful in the design and production of high-performance solid electrolytes. [8].

2. MATERIALS AND METHODS

2.1 Silica Production from Rice Husk

The greyish powder of rice husk ash silica ($RHASiO_2$) derived from the uncontrolled burning of rice milling in Muar Johor, Malaysia, at a temperature rate of roughly 450 °C. The powders were calcined at 700 °C before being added to SDC, and then undergoing dry ball-milling process for 3 hours to get the cleanest and smallest practicable particle size (between 0.1-0.6 μm). SDC was obtained commercially (from Korea's Kceracell). SDC and $RHASiO_2$ powders were mixed for 3 hours with 200 rpm speed in a low-speed ball-milling procedure with different $RHASiO_2$ composition to produce four types of SDC-$RHASiO_2$ powder samples: SDC0, SDC0.25, SDC0.5, and SDC1.0, which contain 0%, 0.25%, 0.5%, and 1.0%

$RHASiO_2$. A uniaxial press was used to make the SDC-$RHASiO_2$ composite pellets with 30 mm diameter and 1 mm thickness. The pellets were then sintered for 60 minutes at 1200 °C.

2.2 Characterizations of Rice Husk Silica

In order to investigate the different reaction steps and temperature of the prepared powder, a differential thermal analyzer and a thermogravimetric analyzer (DTA & TGA, Model: SDT2960 Simultaneous DTA-TGA) with a heating rate of 10 °C/min in air were used. The Archimedes technique was used to determine the densities and porosities of the sintered pellets. The functional groups in the sample were identified using a Thermo Scientific FTIR Nicolet 6700 equipped with an attenuated total reflectance (ATR) accessory. The spectra were collected using 32 scans at 4 cm^{-1} resolution in the 4000-400 cm^{-1} range. The scanning electron microscope SEM (Hitachi, SU1510, Japan) was used to analyze the cross-sectional morphology of RHA powder. Energy dispersive X-ray (EDX) was used to determine the element distribution in the composite. To improve accuracy and precision, picture J analysis was utilized to detect the porosity values from the thin section picture. As a result of this improvement in the color palette, along with greater resolution and more complete photography of the microporosity, the true area that the computer will threshold as pore space will improve.

3. RESULTS AND DISCUSSION

3.1 Thermal Characterization (TGA) of SDC-$RHASiO_2$

Figure 1 illustrates TGA graphs of weight loss for various SDC-$RHASiO_2$ composite compositions. The temperature was plotted against the weight loss, which represented the delta mass (mg). The first mass loss appeared at 100 °C was due to the removal of physisorbed moisture. The second weight loss between 110 °C and 250 °C was caused by the dehydration of hydroxyl groups in PVA polymer intra or inter chains. The third weight loss between 400 °C and 550 °C was related to the decomposition of the polymer chains and the acetate salts. Almost no weight loss was observed after 550 °C indicating metal oxide formation. However, the calcination of the fibers was realized at 800 °C in order to ensure that no carbon residue remained on the samples.

The graph was created to detect the weight loss of four separate samples (SDC0, SDC0.25, SDC0.5, and SDC1.0), which can be seen when the sintering temperature increases. Ceria-based materials can undergo phase transitions at high temperatures. The phase transition involves changes to the crystal structure, which may result in porosity alterations and weight loss. In the case of SDC-$RHASiO_2$, the Si element has an effect on the temperature and crystallinity behavior.

3.2 Porosity of SDC-$RHASiO_2$

Table 1 shows the apparent density and percentage of apparent porosity determined using the Equations 1 and 2, indicating a considerable reduction in porosity in pellets with the addition of $RHASiO_2$.

$$Apparent\ Density = \frac{W_d}{W_w - W_s} \quad (1)$$

$$Percentage\ of\ Apparent\ Porosity = \frac{W_w - W_d}{W_w - W_s} \quad (2)$$

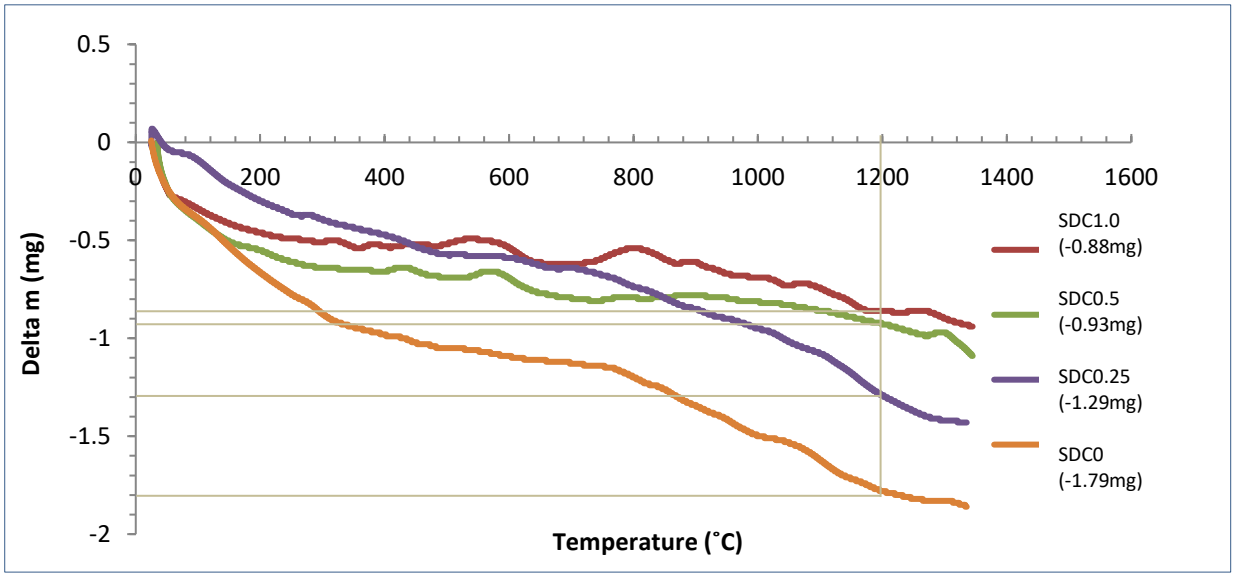

Figure 1: Thermal behaviour for SDC-RHASiO$_2$ electrolyte

Table 1: Apparent density and percentage of apparent porosity for SDC-RHASiO$_2$ electrolyte

Samples	Apparent density (g/mm^3)	Percentage of apparent porosity (%)
SDC0	3.885	5.215
SDC0.25	3.949	4.996
SDC0.5	3.974	4.944
SDC1.0	4.074	4.893

Apparent density for SDC1.0 is the highest (4.074 g/mm^3) followed by SDC0.5 (3.974 g/mm^3), SDC0.25 (3.949 g/mm^3) and lastly SDC0 (3.885 g/mm^3). On the other hand, percentage of apparent porosity tabulated shows that porosity is the highest with SDC0 (5.215%) followed by SDC0.25 (4.996%), SDC0.5 (4.944%) and SDC1.0 (4.893%) coming last. Based on the result obtained, the existence of RHASiO$_2$ in SDC pallet helps to reduce porosity which improving the densification of electrolyte composites. Figure 2 shows the graph of apparent density and percentage of apparent porosity for SDC-RHASiO2 electrolyte. The apparent density of the samples increases as the weight percentage of RHASiO$_2$ added to SDC increases. As for apparent porosity, pellets with higher RHASiO$_2$ weight percentage have lower percentage of apparent porosity. These situations occur due to the RHASiO$_2$ particles occupy the space between SDC particles and cause the SDC become denser and compact [9]. This theory can be proved with the SEM result from Figure 4. The reduction of porosity makes better electrolyte composite.

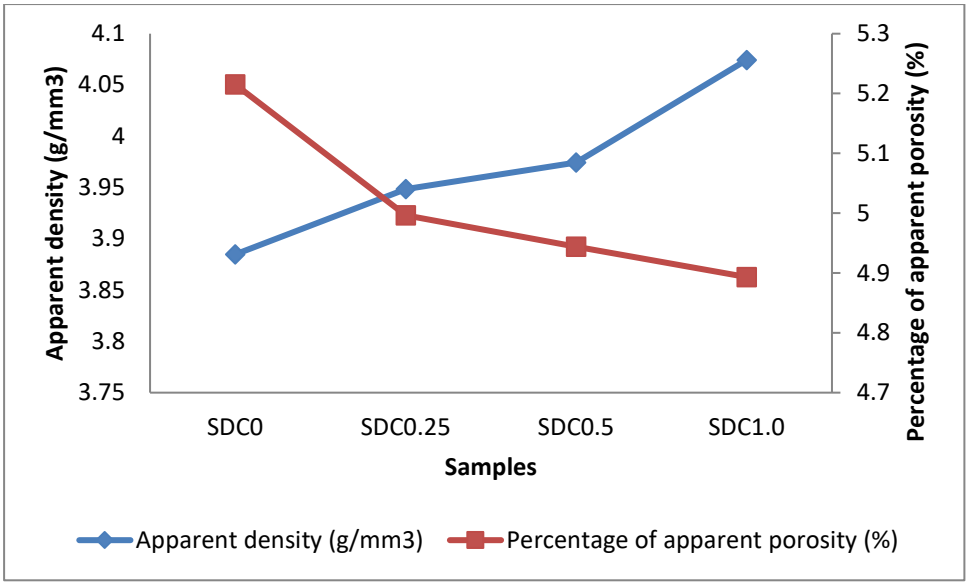

Figure 2: Graph apparent density and percentage of apparent porosity for SDC-RHASiO_2 electrolyte

3.3 Chemical Bonding Analysis of SDC-RHASiO_2

Figure 3 shows IR spectra obtained under group CeO stretching frequencies in the range of wavenumbers between 900-1300 cm^{-1} and SiO_2 asymmetric stretching vibrations in the region of wavenumbers between 1000-1100 cm^{-1}. Each composition displays a composite at four distinct compositions. It is critical to determine the functional group of organic compounds by analyzing infrared ray transmittance lines.

Based on Table 2, it is clear that the addition of silica to the composite will result in the inclusion of new elements, and that raising the sintering temperature will most likely result in the addition of new bonding elements in the SDC-RHASiO_2 composite electrolyte pellets [10-12].

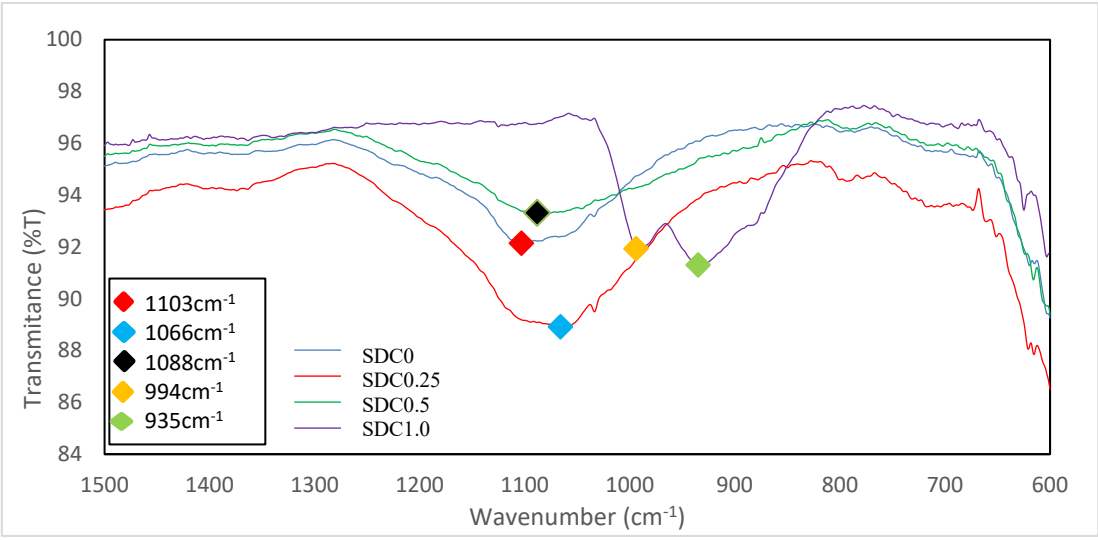

Figure 3: FTIR spectra of SDC-RHASiO_2 electrolyte

Table 2: Band assignments of SDC-RHASiO$_2$ electrolyte

Wavelength (cm^{-1})	Band Assignments	Wavelength Range(cm^{-1})	References
935, 994, 1088, 1066, 1103	Ce-O Stretching frequency	900-1300	[13]
1088, 1066, 1103	Si-O-Si Asymmetric stretching vibration	1000-1100	[14]

3.4 Morphology and Element Analysis of SDC-RHASiO$_2$

The constituents of the SDC-RHASiO$_2$ composite electrolyte pellets with four distinct compositions were evaluated by EDX are shown in Figure 4.

Samples	Microstructure and Porosity Area	Elemental Composition (%)			Porosity Average Value, %Area
SDC0	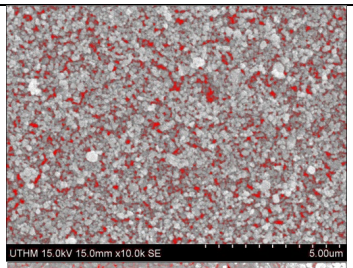	Element	Weight%	Atomic%	5.13
		O	21.08	70.12	
		Ce	67.46	25.80	
		Sm	11.46	4.08	
		Total	100.00		
SDC0.25	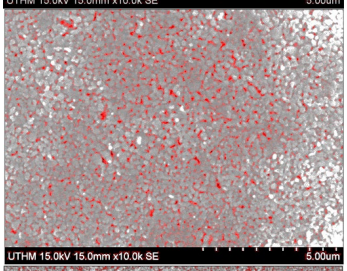	Element	Weight%	Atomic%	4.97
		O	19.72	68.28	
		Si	0.17	0.34	
		Ce	60.09	27.32	
		Sm	11.02	4.06	
		Total	100.00		
SDC0.5	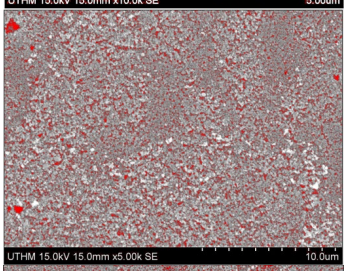	Element	Weight%	Atomic%	4.89
		O	21.20	70.17	
		Si	0.27	0.50	
		Ce	64.80	24.49	
		Sm	13.73	4.84	
		Total	100.00		
SDC1.0	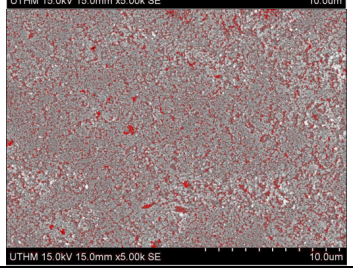	Element	Weight%	Atomic%	4.75
		O	23.00	71.58	
		Si	0.94	1.67	
		Ce	65.06	23.12	
		Sm	10.99	3.64	
		Total	100.00		

Figure 4: SEM images of surface morphology and porosity value through the ImageJ software for SDC-RHASiO$_2$ electrolyte

The essential ingredients in composite electrolyte pellets manufactured from the SDC-$RHASiO_2$ combination are samarium (Sm), ceria (Ce), oxygen (O), and silicon (Si). For SDC0.25, SDC0.5, and SDC1.0, all of these critical components are present in the SDC-$RHASiO_2$ composite electrolyte pellets.The highest proportions of (Ce) components were found in SDC-$RHASiO_2$ composite electrolyte pellets, followed by (O), (Sm), and finally (Si). The lower the quantity of silica content measured in the composite, the less $RHASiO_2$ added.

Image J was used to examine the porosity values acquired from the SEM results. To improve accuracy and precision, the porosity may be detected from the top surface section picture. As indicated in the chart in Figure 4, the true area that the computer would threshold as pore space will improve as a consequence of this improvement in the color palette combined with greater resolution and more complete photography of the micro porosity. To distinguish it from the overall top surface Image J, the porosity was colored red. The existence of porosity and hole in the SDC-$RHASiO_2$ composite electrolyte was shown by red dots. As a consequence, the porosity number will be more accurate and in line with the samples' total porosity [15–17].

The presence of silica influences the porosity of the SDC-$RHASiO_2$ composite electrolyte (Figure 4). As the composition of $RHASiO_2$ been added into SDC increased, the porosity of the SDC-$RHASiO_2$ electrolyte decreased, which reduced the sintering temperature for the electrolyte.

4. CONCLUSIONS

Based on the tests and analysis, it can be determined that adding $RHASiO_2$ to the SDC electrolyte improves its characteristics significantly. Higher density in electrolytes with higher $RHASiO_2$ weight percentages implies increased compactness and potential for better performance in electrochemical applications. Furthermore, the FTIR data show that $RHASiO_2$ has successfully bonded to the SDC matrix, validating its incorporation into the composite. The presence of SiO, as determined by EDX analysis, supports the inclusion of silica as a novel bonding element, which contributes to the composite's overall stability. Furthermore, increasing $RHASiO_2$ composition results in a decrease in porosity as seen in SEM micrographs and Image J analysis, indicating increased structural integrity. Therefore, the comprehensive findings support the conclusion that incorporating $RHASiO_2$ into SDC results in a composite with decreased porosity and enhanced properties, thus holding promise for various practical applications.

Acknowledgements

The author gratefully acknowledges the financial support provided by Malaysia Ministry of Higher Education (MOHE) through Fundamental Research Grant Scheme (FRGS) - K317, and Research Management Centre (RMC), Universiti Tun Hussein Onn Malaysia (UTHM) for managing our research grant.

Author Contributions

All authors contributed toward data analysis, drafting and critically revising the paper and agree to be accountable for all aspects of the work.

Disclosure of Conflict of Interest

The authors have no disclosures to declare

Compliance with Ethical Standards

The work is compliant with ethical standards

References

[1] Zolhafizi, J., Azmi, M. A., Rahman, H. A., Zakaria, H., Hassan, S., Mahzan, S., Ismail, A., Ariffin, A. M. T., Tukimon, M. F, Yusof, U. A. & Baharuddin, N. A. (2023). Samarium doped ceria (SDC) electrolyte modification by sintering aids addition to reducing sintering temperature: A Review. *Jurnal Kejuruteraan*, 35(1),65-76.

[2] Xu, Q. (2023). Modelling of High Temperature Methanol-Fuelled Solid Oxide Fuel Cells. (Ph.D. Thesis, Hong Kong Polytechnic University, China), pp. 1-15.

[3] Tian, Y., Abhishek, N., Yang, C., Yang, R., Choi, S., Chi, B., Pu, J., Ling, Y., Irvine, J. T. & Kim, G. (2022). Progress and potential for symmetrical solid oxide electrolysis cells. *Matter*, 5(2), 482-514.

[4] Winck, L. B., de Almeida Ferreira, J. L., Martinez, J. M. G., Araujo, J. A., Rodrigues, A. C. M. & da Silva, C. R. M. (2017). Synthesis, sintering and characterization of ceria-based solid electrolytes codoped with samaria and gadolinium using the Pechini method. *Ceramics International*, 43(18), 16408-16415.

[5] Panthi, D., Hedayat, N. & Du, Y. (2017). A comparative study on the densification behavior of yttria-stabilized zirconia electrolyte powders. *ECS Transactions*, 78(1), 327.

[6] Hussain, S. & Yangping, L. (2020). Review of solid oxide fuel cell materials: cathode, anode, and electrolyte. *Energy Transitions*, 4(2), 113-126.

[7] Wain-Martin, A., Morán-Ruiz, A., Laguna-Bercero, M. A., Campana, R., Larranaga, A., Slater, P. R. & Arriortua, M. I. (2019). SOFC cathodic layers using wet powder spraying technique with self-synthesized nanopowders. *International Journal of Hydrogen Energy*, 44(14), 7555-7563.

[8] Jaidi, Z., Azmi, M. A., Abd Rahman, H., Huai, T. K., Yusop, U. A., Ghani, M. Z. I. A. & Roslan, M. F. (2023). The effect of milling duration to the structural properties of silica from rice husk. *Malaysian Journal of Microscopy*, 19(1), 193-201.

[9] Zhang, L., Jiang, Y., Zhu, K., Shi, N., Chen, Z., Peng, R. & Xia, C. (2024). Fe-doped SDC solid solution as an electrolyte for low-to-intermediate-temperature solid oxide fuel cells. *ACS Applied Materials & Interfaces*, 16(4), 4648-4660.

[10] Rout, S. K. & Pratihar, S. K. (2021). Tailoring of properties in the preparation level of nano crystalline Ce0. 8Sm0. 2O1. 9-δ (SDC) for the use of SOFC electrolyte. *Materials Today: Proceedings*, 45, 5764-5768.

[11] Zaman, S. W. Z. S., Rahman, N. F. A. & Rahman, H. A. (2021). Characterization and review of dual composite cathodes LSCF-SDC / YSZ-SDC for intermediate to low temperature solid oxide fuel cell. *Research Progress in Mechanical and Manufacturing Engineering,* 2(2), 1–10.

[12] Rahman, N. F. A., Ismail, A., Azmi, M. A., Mahzan, S. & Rahman, H. A. (2022). Phase stability of LSCF/YSZ-SDC & LSCF/YSZ-SDCC dual composite cathode solid oxide fuel cell. *Research Progress in Mechanical and Manufacturing Engineering*, 3(1), 1065-1074.

[13] Kundu, S., Sutradhar, N., Thangamuthu, R., Subramanian, B., Panda, A. B. & Jayachandran, M. (2012). Fabrication of catalytically active nanocrystalline samarium (Sm)-doped cerium oxide (CeO_2) thin films using electron beam evaporation. *Journal of Nanoparticle Research*, 14, 1-16.

[14] Azmi, M. A., Ismail, N. A. A., Rizamarhaiza, M. & Taib, H. (2016). Characterisation of silica derived from rice husk (Muar, Johor, Malaysia) decomposition at different temperatures. *AIP Conference Proceedings,* 1756(1), 020005.

[15] Muda, R., Ahmad, S., Azmi, M. A., Taib, N. & Taib, H. (2019). Characterisation of silica derived from rice husk ash and nickel oxide at different composition and temperatures. *International Journal of Materials and Product Technology*, 59(2), 91-101.

[16] Abubakar, M., Muthuraja, A., Rajak, D. K., Ahmad, N., Pruncu, C. I., Lamberti, L. & Kumar, A. (2020). Influence of firing temperature on the physical, thermal and microstructural properties of kankara kaolin clay: a preliminary investigation. *Materials*, 13(8), 1872.

[17] Shaari, N. & Kamarudin, S. K. (2019). Current status, opportunities, and challenges in fuel cell catalytic application of aerogels. *International Journal of Energy Research*, 43(7), 2447-2467.